Comparison of the dielectric function of AlPd, Al_3Pd, and $Al_{70}Pd_{20}Mn_{10}$ determined by electron-energy-loss measurements

M. Zurkirch, M. DeCrescenzi,* and M. Erbudak
Laboratorium für Festkörperphysik, Eidgenössische Technische Hochschule Zürich, CH-8093 Zürich, Switzerland

A. R. Kortan
Bell Laboratories, Lucent Technologies, Murray Hill, New Jersey 07974
(Received 6 May 1997)

Electron-energy-loss measurements on crystalline AlPd and Al_3Pd as well as on quasicrystalline $Al_{70}Pd_{20}Mn_{10}$ are evaluated in terms of optical constants using the Kramers-Kronig analysis. Interband transitions in AlPd are identified, and found to be in agreement with those obtained from the theoretical density of states, whereas spectra of Al_3Pd are dominated by plasmon excitations due to the quasifree electrons of Al. For $Al_{70}Pd_{20}Mn_{10}$, the optical properties are strikingly similar to those of AlPd, except for an additional low-energy transition due to the Mn d-derived states, manifesting a predominant Al-Pd interaction in the quasicrystal. [S0163-1829(97)06040-2]

After the discovery of quasicrystals (QC's) in 1984, most of the theoretical and experimental investigations were focused on their very peculiar structural features. It was not before the development of thermodynamically stable QC's at the end of the 1980's that some effort was made to scrutinize their electronic and optical properties. Consequently, the question of the extent to which these properties can distinguish between periodic and quasiperiodic structures has been a central topic in recent years. The electronic structure of $Al_{70}Pd_{20}Mn_{10}$ has been investigated by means of photoemission[1,2] and soft-x-ray spectroscopy,[3] as well as x-ray photoelectron (XPS) and electron-energy-loss spectroscopy (EELS).[4] These studies have shown certain similarities between the valence bands of crystalline AlPd and those of icosahedral $Al_{70}Pd_{20}Mn_{10}$.[2,4] A more elaborate study has revealed AlPd and $Al_{70}Pd_{20}Mn_{10}$ to possess strikingly similar electronic properties, i.e., almost identical shapes and energy shifts of valence bands[5] as well as of Pd core levels.[4] This indicates that it is not the long-range order but the short-range properties that have a crucial impact on the electronic structure of such alloys. Moreover, it was realized that no features of the electronic structure can exclusively be related to QC's.

The aim of this paper is to present information on the electronic structure of quasicrystalline $Al_{70}Pd_{20}Mn_{10}$ as well as crystalline AlPd and Al_3Pd, derived from EELS measurements in an energy region of 1–50 eV using the Kramers-Kronig (KK) analysis. It is found that the electronic properties for AlPd and $Al_{70}Pd_{20}Mn_{10}$ are largely dictated by the $4d$ bands of Pd and, hence, are very similar. In QC's, transitions due to Mn-derived states are identified. Although no evidence could be found for the quasifree behavior of the Al-derived electrons, the shape of the dielectric constant of $Al_{70}Pd_{20}Mn_{10}$ unambiguously suggests a metallic character. In Al_3Pd, on the other hand, all features due to interband transitions are obscured by plasmon oscillations, thus indicating that the free-electron behavior of Al-Pd alloys depends mainly on the composition and not on the crystalline structure.

The experiments were performed in an ultrahigh-vacuum (UHV) chamber with a total pressure in the lower 10^{-9}-Pa region. The macroscopic-sized samples, i.e., 10×7 and 9×8 mm^2 for the crystalline AlPd and Al_3Pd, respectively, and 6×4 mm^2 for the quasicrystalline $Al_{70}Pd_{20}Mn_{10}$, were grown by conventional techniques.[6] The polycrystalline AlPd sample was in its high-temperature β phase, that has a CsCl structure.[5] For Al_3Pd, a structural model has been suggested recently to be closely related to decagonal QC's with a period of about 1.6 nm.[7] For $Al_{70}Pd_{20}Mn_{10}$, on the other hand, at least 60% of the atoms in the unit formula are situated in clusters. These are the so-called Mackay clusters composed of two shells: a small icosahedron and a larger icosidodecahedron.[8,9] After inserting the samples into UHV, the surfaces were cleaned by sputtering with Ar^+ (1500 eV, 0.1 μA/mm^2) until the contamination with oxygen and carbon was below the limits of detectability of XPS, i.e., for 15 min typically. For the XPS measurements an unmonochromatized Al K_α-radiation source was used. The electron gun employed for EELS delivered a beam focused on the specimen to a spot size of 0.3 mm. For the measurements reported here, the primary-electron energy (E_p) was set to 1500 eV to ensure that the inelastic cross section was comparable to that of the photoelectrons considered. The total energy resolutions for XPS and EELS were 1.0 and 0.7 eV, respectively. The details of the apparatus can be found elsewhere.[4]

After sputtering and annealing, the surface composition of the samples was determined by comparing the ratio of the Pd $3d$- and the Al $2p$-emission intensities in XPS for the pure metals with those in the alloys. It was found that the surfaces of AlPd and Al_3Pd have nominal bulk compositions. For $Al_{70}Pd_{20}Mn_{10}$, however, the concentration of Pd at the surface was found to be higher than expected with respect to the bulk concentration. In fact, the composition was similar to that of AlPd. However, patterns of secondary-electron imaging obtained from this surface clearly display the existence of twofold-, threefold-, and fivefold-symmetry axes.[8] This fact proves that as a consequence of the Pd enrichment the

surface of $Al_{70}Pd_{20}Mn_{10}$ does not revert to the CsCl structure typical of AlPd, but remains quasicrystalline, displaying the icosahedral symmetry elements of the bulk. The surface thus prepared was recently compared with AlPd using XPS and secondary-electron imaging.[4,5] However, at the surface of $Al_{70}Pd_{20}Mn_{10}$ we have observed a transition from quasicrystal to CsCl structure upon prolonged sputtering for 2 h. The composition did not change any further due to this treatment. At this stage, the surface of the quasicrystal is covered with a crystalline layer which is structurally and electronically identical to AlPd. The quasicrystalline structure and the nominal bulk composition can be restored by subsequent annealing at 700 K for more than an hour.[10] Similar phase transitions from the quasicrystalline state to the $B2$-type phase have already been observed upon irradiation with a high-energy Ar-ion beam.[11]

In EELS, performed in reflection mode, the cross section $N(E)$ for inelastic scattering (absorption) is dominated by those scattering processes for which the magnitude of the momentum transfer (q) is minimal, i.e., $q=q_{\min}$.[12] If, additionally, the momentum transfer $q_{\min}$ involved in the electronic transitions is negligibly small, then the dipole approximation generally applied in optics can (as a simplification) be extended to inelastic electron scattering. Due to the reflection geometry, however, the cross section for electron absorption has to be discussed in terms of surface and bulk contributions:[13,14]

$$N(E)\simeq S\left(-\mathrm{Im}\frac{1}{1+\epsilon(\omega)}\right)+B\left(-\mathrm{Im}\frac{1}{\epsilon(\omega)}\right),$$

where S and B are two weighting functions that depend on the energy of the primary electrons and thereby on the mean free path of the secondary electrons emitted. Under these conditions a direct link between electron-energy-loss spectra and the dielectric function $\epsilon(\omega)=\epsilon_1+i\epsilon_2$ is provided through the KK relation.[15] For the present measurements, considering that $q_{\min}\propto\sqrt{E_p}-\sqrt{E_p-\Delta E}$ and $E_p=1500$ eV, we obtain for the energy loss ΔE in the range of 5–30 eV, a $q_{\min}$ in the range of 0.04 and 0.18 Å^{-1}. This value is negligibly small, and hence the applicability of the dipole approximation is justified.

Figure 1 shows an EELS spectrum of pure Pd together with ϵ_1 and ϵ_2 derived from the experimental curve using the KK analysis. The electronic properties of Pd have been studied thoroughly, yet we show our data in order to illustrate the procedure we applied for the investigation of the electronic and optical properties of the alloys. The curve designated as ''theory'' was obtained from a convolution of the occupied and unoccupied density of states (DOS) as calculated by Lässer and Smith.[16] According to this work, features $a-d$ at 4.6, 13.3, 19.5, and 30.7 eV, respectively, correspond to interband transitions from initial bands below the Fermi level E_F, to final states above E_F. The initial states have predominantly d character and the final states sp character. Therefore, the structures observed in ϵ_2 reflect the enhanced values of the joint DOS at different critical points in $\mathbf{k}$ space. The main peaks in EELS, i.e., $A-D$, which occur at energies where the absorption is low, i.e., 6.4, 14.8, 24.0, and 31.8 eV, respectively, are interpreted as collective oscillations, which are in competition with the interband

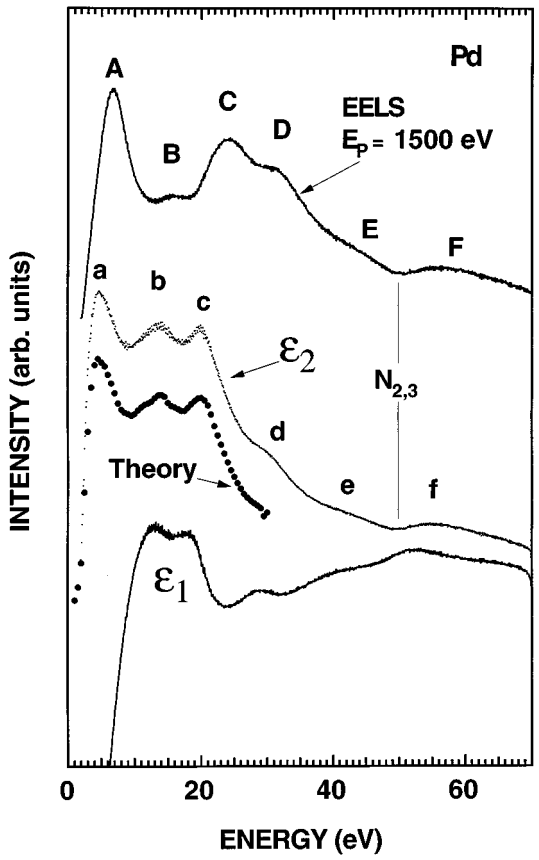

FIG. 1. EELS results (top) for pure Pd acquired at a primary energy of 1500 eV. The dielectric constant (ϵ_1,ϵ_2) is derived from this experimental curve using the KK analysis. ϵ_2 is compared with the joint DOS (marked ''theory'') obtained by the convolution of theoretical band-structure data (Ref. 16). The abscissa represents the loss energy for the experimental and the excitation/absorption energy for the other curves.

transitions.[12,17,18] Thus it can be assumed as a practical rule that maxima of ϵ_2 coincide with minima of the loss function, or, in other words, $N(E)\propto-\mathrm{Im}(1/\epsilon)\propto 1/\epsilon_2$. In contrast, features F and f are at the same position because they are generated by an inner-shell transition from the Pd $N_{2,3}$ $(4p)$ core levels. In fact, in this energy-loss region $(\Delta E\geqslant 20$ eV), ϵ_2 is small and ϵ_1 nearly constant. Hence the loss function mimics ϵ_2.

According to a recent study,[5] the electronic structure of $Al_{70}Pd_{20}Mn_{10}$ is very close to that of AlPd. The energy position and the spectral shape of their valence bands are very much alike, apart from a contribution from Mn at E_F. In order to shed more light on the electronic structure of these two alloys, EELS and ϵ_2 data are shown in Fig. 2. The most salient features in EELS occur for both alloys at energies of 2.8 eV (A and A'), 5.5 eV (B and B'), and at 19.5 and 18 eV (C and C', respectively). The curves representing ϵ_2, on the other hand, display absorption peaks at 2 eV (a and a'), 4 eV (b and b'), and 8.5 eV (c and c'). In the computed data, obtained from a convolution of tight-binding linear-muffin-tin-orbital (TB-LMTO) calculations for AlPd (Ref. 19) and labeled ''theory,'' peaks b' and c' are satisfactorily reproduced. This, in combination with recent XPS measurements,[4] suggests that features b (b') and c (c'), present in both

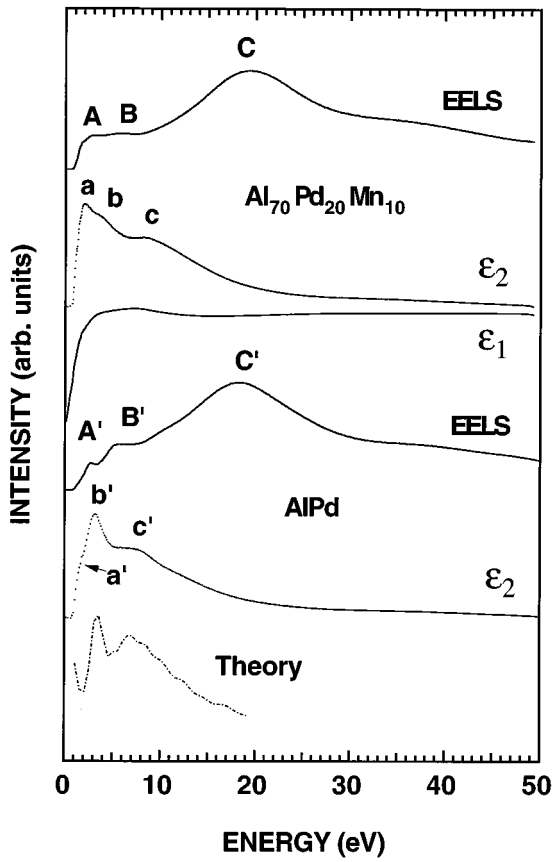

FIG. 2. EELS data at $E_p = 1500$ eV obtained from $Al_{70}Pd_{20}Mn_{10}$ (top) compared to those for AlPd. Also shown are the ϵ_1 and ϵ_2 curves obtained by the KK analysis. The curve, labeled ''theory,'' is a joint DOS for AlPd derived from TB-LMTO calculations (Ref. 19). The abscissa represents the loss energy for the experimental data and the excitation and/or absorption energy for the other curves.

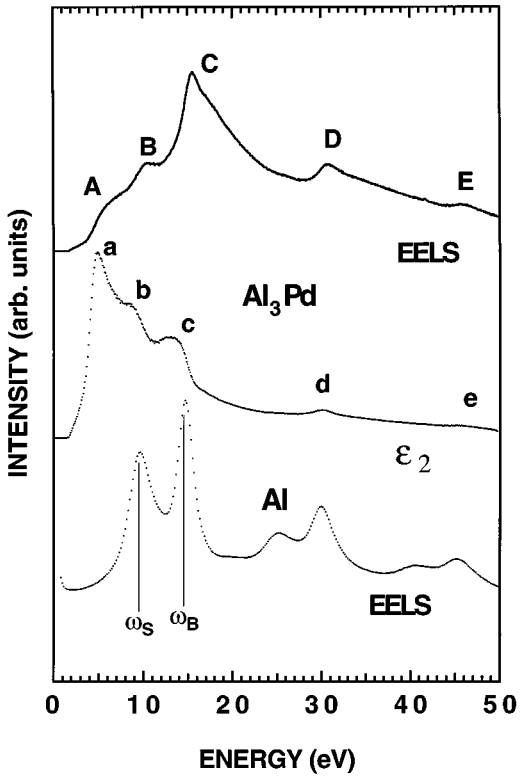

FIG. 3. Direct comparison of the collective oscillations in Al_3Pd and pure Al by means of EELS measured at a primary energy of 1500 eV. The frequency of the bulk and the surface plasmons in Al are marked with ω_B and ω_S, respectively. Also shown is the ϵ_2 curve for Al_3Pd obtained by the KK analysis and drawn on the same energy scale.

alloys, are generated by interband transitions at the Pd site. In addition to the overlap of the spectra for the two materials, there is at least one main difference that deserves comment, namely, the absorption peak a at 2 eV, which is much stronger $Al_{70}Pd_{20}Mn_{10}$ than for AlPd. As there are Mn states very close to the E_F,[1,3,5] this increase in intensity is certainly due to transitions of Mn electrons from bonding to antibonding states. Another point to emphasize is the correspondence between the absorption peaks ($a-c$) and the collective oscillations ($A-C$) that follow them, confirming the validity of the interpretation scheme established for pure Pd. For $Al_{70}Pd_{20}Mn_{10}$, ϵ_1 is also shown in the same figure in order to emphasize the metallic behavior of the quasicrystalline sample.

Figure 3 shows EELS measurements obtained from Al_3Pd and pure Al in order to demonstrate that the electronic excitations in Al_3Pd are dominated by Al plasmons. Also shown is the calculated loss function ϵ_2 for Al_3Pd, derived from the EELS data using the KK analysis. The most pronounced features for Al_3Pd are situated at distinctly different energy positions, i.e., at 7, 10, 15.5, 30, and 46 eV in EELS, labeled $A-E$, and at 5, 8.5, 13.5, and 30.5 eV in ϵ_2, labeled $a-e$. The EELS spectrum for pure Al shows predominantly bulk and surface plasmon excitations, marked ω_B and ω_S, respectively. The surface plasmon at 10 eV, the bulk plasmon at 15.5 eV, and their higher harmonics dominate the loss data. By comparison with the spectrum for pure Al, all loss features in Al_3Pd can be identified as plasmon losses, except for the low-energy peak A, which represents an interband transition. However, other features due to Pd interband transitions, illustrated in Fig. 1, are completely masked. It is interesting to note that the energy values for plasmon losses in Al_3Pd are very close to those in pure Al. In fact, the value for the bulk plasmon is shifted by approximately 0.5 eV to higher energy in Al_3Pd. This change corresponds to an increase of about 6% in the density of excitable quasifree electrons in going from Al to the alloy.

In order to investigate the individual contributions of Al and Pd atoms in the Al_3Pd alloy to the measured EELS spectrum, XPS measurements are performed in an extended region of core levels, and satellite structures are determined. A core-level spectrum is a local probe at a particular atomic site and is chemically sensitive. Figure 4 presents XPS spectra for the Al $2s$ core level and the valence band of Al_3Pd. The latter consists predominantly of Pd-derived $4d$ electrons. The centroids of both emission lines are set to zero energy, which facilitates the observation of the different energy positions of the satellites accompanying these lines. While the Al $2s$ emission is followed by a feature at 15.5 eV, which apparently corresponds to a plasmon loss, the valence band has a satellite at 19 eV, the origin of which is an interband transi-

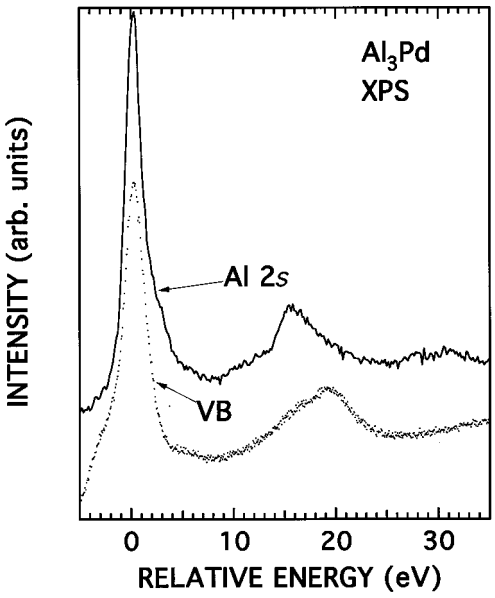

FIG. 4. XPS results from the valence band (bottom) and the Al $2s$ core level (top) of Al_3Pd. The abscissa represents the relative energy, i.e., zero is placed at the centroid of the Pd $4d$ states for the valence-band emission and at the binding energy of the Al $2s$ component for the curve at the top.

tion involving the Pd $4d$ electrons. Hence, in the same alloy, there is a coexistence of free-electron behavior associated with Al and single-electron transitions at the Pd site. The loss process at the Pd site is neither observable as a feature in EELS, nor as a peak in ϵ_2, because of the dominant occurrence of the Al plasmons. In AlPd and $Al_{70}Pd_{20}Mn_{10}$, on the other hand, no satellites could be found accompanying the Al $2s$ emission lines due to the lack of plasmon excitations.[4,5] Although very similar in their nominal compositions, a further difference between $Al_{70}Pd_{20}Mn_{10}$ and Al_3Pd is the binding energy of their valence bands. Hence $Al_{70}Pd_{20}Mn_{10}$ has electronic properties similar to AlPd, but not to Al_3Pd.

While the $4d$ band of palladium is located at E_F in the pure metal, it moves to higher binding energies in the alloys due to hybridization with Al sp electrons. Thus, the centroids of the valence band are found at 3.9 eV for both AlPd (Refs. 5 and 20) and $Al_{70}Pd_{20}Mn_{10}$,[5] and at 4.8 eV for Al_3Pd.[20] Based on this information about the occupied states, we can infer the character of the available final states in Pd and the alloys by inspecting the dielectric function ϵ_2. Thus, peak a for Pd corresponds to transitions of the $4d$ electrons to states about 4.6 eV above E_F. This transition is shifted to higher excitation energies in AlPd and $Al_{70}Pd_{20}Mn_{10}$ (peaks c and c' in Fig. 1 at 8.5 eV) due to the energy shift of the initial $4d$ states. Then, within the present assumptions, the final states remain at the same energy in going from pure Pd to these alloys. Similarly, peaks b and b' in Fig. 1 at 4.0 eV are produced by transitions of the $4d$ bands to states at E_F, and peak a by transitions at the Mn site.

In summary, the electronic excitations in Al_3Pd were observed to be totally dominated by Al plasmons, which obscure the single-particle interband transitions. A strong resemblance of the electronic properties in an extended region could be verified for AlPd and $Al_{70}Pd_{20}Mn_{10}$. This similarity indicates that the same average number of a particular atomic species might be expected around a specific site, i.e., a very similar short-range order. In quasicrystalline $Al_{70}Pd_{20}Mn_{10}$ there is possibly a strong interaction between Al and Mn atoms, leading to a hybridization of Mn $3d$-derived states and Al sp states, giving rise to a band structure similar to that of AlPd instead of Al_3Pd. The lack of Al plasmons in AlPd, which is a periodic structure, as well as in quasicrystalline $Al_{70}Pd_{20}Mn_{10}$, implies that not so much the long-range atomic arrangement, but the composition is responsible for the free-electron behavior in Al-Pd alloys. Similarly, a recent low-energy electron-diffraction study on $Al_{70}Pd_{21}Mn_9$ could reproduce the experimental data with calculations assuming a layered structure for QC's consisting of a top Al layer, mixed with about 10% Mn, and a second layer containing one-to-one Al and Pd with only small amounts of Mn.[21]

Finally, no energy gap could be found in $Al_{70}Pd_{20}Mn_{10}$. According to ϵ_1, it clearly has a metallic character. Recent high-resolution ultraviolet-photoemission measurements have confirmed a possible gap to be smaller than 6 meV.[22] It is possible, however, that the existence of such a small gap in the DOS at E_F has no sizable impact on the optical constants. In order to treat this phenomenon more accurately infrared measurements or high-resolution EELS would be required.

Special thanks go to R. Monnier for performing the TB-LMTO calculations of the DOS of AlPd, and to D. D. Vvedensky for fruitful discussions. One of us (M.Z.) is grateful to the Eidgenössische Technische Hochschule Zürich for financial support.

*Permanent address: Dipartimento di Matematica e Fisica, Unità di Ricerca INFM, Università di Camerino, I-62032 Camerino, Italy.

[1] G. W. Zhang, Z. M. Stadnik, A.-P. Tsai, and A. Inoue, Phys. Lett. A **186**, 345 (1994).

[2] G. W. Zhang, Z. M. Stadnik, A.-P. Tsai, and A. Inoue, Phys. Rev. B **50**, 6696 (1994).

[3] E. Belin and Z. Danhkázi, J. Non-Cryst. Solids **153/154**, 298 (1993).

[4] M. Zurkirch, A. Atrei, M. Hochstrasser, M. Erbudak, and A. R. Kortan, J. Electron Spectrosc. Relat. Phenom. **77**, 233 (1996).

[5] M. Zurkirch, M. DeCrescenzi, M. Erbudak, M. Hochstrasser, and A. R. Kortan, Phys. Rev. B **55**, 8808 (1997).

[6] A. R. Kortan, F. A. Thiel, H. S. Chen, A. P. Tsai, A. Inoue, and T. Masumoto, Phys. Rev. B **40**, 9397 (1989).

[7] Y. Matsuo and K. Hiraga, Philos. Mag. Lett. **70**, 155 (1994).

[8] M. Zurkirch, M. Erbudak, H.-U. Nissen, M. Hochstrasser, E. Wetli, and S. Ritsch, Philos. Mag. Lett. **72**, 199 (1995).

[9] M. Boudard, M. de Boissieu, C. Janot, G. Herger, C. Beeli, H.-U. Nissen, H. Vincent, R. Ibberson, M. Audier, and J. M. Dubois, J. Phys.: Condens. Matter **4**, 10 149 (1992).

[10] M. Zurkirch *et al.* (unpublished).

[11] X. Yang, R. Wang, and X. Fan, Philos. Mag. Lett. **73**, 121 (1996).

[12] G. Chiarello, E. Colavita, M. DeCrescenzi, and S. Nannarone, Phys. Rev. B **29**, 4878 (1984).

[13] E. Colavita, M. DeCrescenzi, L. Papagno, R. Scarmozzino, L. S. Caputi, R. Rosei, and E. Tosatti, Phys. Rev. B **25**, 2490 (1982).

[14] F. Yubero and S. Tougaard, Phys. Rev. B **46**, 2486 (1992).
[15] Y. Ohno, Phys. Rev. B **39**, 8209 (1989).
[16] R. Lässer and N. V. Smith, Phys. Rev. B **25**, 806 (1989).
[17] J. Daniels, C. von Fenstenberg, M. Raether, and K. Zeffenfeld, *Optical Constants of Solids By Electron Spectroscopy*, Springer Tracts in Modern Physics Vol. 54 (Springer, New York, 1970).
[18] T. Bornemann, J. Eickmans, and A. Otto, Solid State Commun. **65**, 381 (1988).
[19] R. Monnier (unpublished).
[20] J. C. Fuggle, F. U. Hillebrecht, R. Zeller, Z. Zołnierek, P. A. Bennet, and C. Freiburg, Phys. Rev. B **27**, 2145 (1982).
[21] M. Gierer, M. A. Van Hove, A. I. Goldman, Z. Shen, S.-L. Chang, C. J. Jenks, C.-M. Zhang, and P. Thiel, Phys. Rev. Lett. **78**, 467 (1997).
[22] Z. M. Stadnik, D. Purdie, M. Garnier, Y. Baer, A.-P. Tsai, A. Inoue, K. Edagawa, and S. Takeuchi, Phys. Rev. Lett. **77**, 1777 (1996).